Inferring energy dissipation from violation of the fluctuation-dissipation theorem

Shou-Wen Wang[*]

Beijing Computational Science Research Center, Beijing, 100094, China
and Department of Engineering Physics, Tsinghua University, Beijing, 100086, China

The Harada-Sasa equality elegantly connects the energy dissipation rate of a moving object with its measurable violation of the Fluctuation-Dissipation Theorem (FDT). Although proven for Langevin processes, its validity remains unclear for *discrete* Markov systems whose forward and backward transition rates respond *asymmetrically* to external perturbation. A typical example is a motor protein called kinesin. Here we show generally that the FDT violation persists surprisingly in the high-frequency limit due to the asymmetry, resulting in a divergent FDT violation integral and thus a complete breakdown of the Harada-Sasa equality. A renormalized FDT violation integral still well predicts the dissipation rate when each discrete transition produces a small entropy in the environment. Our study also suggests a way to infer this perturbation asymmetry based on the measurable high-frequency-limit FDT violation.

I. INTRODUCTION

Recent development of technology has allowed direct observation and control of molecular fluctuations, thus opening up a new field to explore nanomachines that operate out of equilibrium [1–3]. An important approach to investigate a stochastic system is to study both its spontaneous fluctuation and the elicited response to perturbation. For the recorded velocity $\dot{x}_t$ of a particle (with x_t being its position at time t), its spontaneous fluctuation is captured by the temporal correlation function: $C_{\dot{x}}(t - \tau) \equiv \langle(\dot{x}_t - \langle\dot{x}\rangle_{ss})(\dot{x}_\tau - \langle\dot{x}\rangle_{ss})\rangle_{ss}$ with $\langle\cdot\rangle_{ss}$ denoting the average over the stationary ensemble. On the other hand, the velocity response to a small external force h is captured by the temporal response function determined from the functional derivative $R_{\dot{x}}(t - \tau) \equiv \delta\langle\dot{x}_t\rangle/\delta h_\tau$. For equilibrium systems, these two functions are closely related through the fundamental Fluctuation-Dissipation Theorem (FDT) [4], which in the Fourier space reads

$$\tilde{C}_{\dot{x}}(\omega) = 2T k_B \tilde{R}'_{\dot{x}}(\omega), \tag{1}$$

where prime denotes the real part, T is the bath temperature, and the Boltzmann factor k_B is set to be 1 hereafter. Violation of the FDT has been widely used to characterize non-equilibrium systems, including glassy systems [5,6], hair bundles [7], and cytoskeleton networks [8].

The generalization of the FDT for systems in non-equilibrium steady state has been studied intensively [9–13]. In particular, for systems described by Langevin equations, Harada and Sasa have shown that the violation integral of the FDT gives the dissipation rate $\dot{q}$ for the observed variable x [14–16]:

$$I \equiv \langle\dot{x}\rangle^2_{ss} + \int_{-\infty}^{\infty}[\tilde{C}_{\dot{x}}(\omega) - 2T \tilde{R}'_{\dot{x}}(\omega)]\frac{d\omega}{2\pi} = \frac{\dot{q}}{\gamma} \tag{2}$$

with γ the friction coefficient. The Harada-Sasa (HS) equality has been applied successfully to infer the energetics of F1-ATPase, a rotary motor protein [17,18]. Our recent study demonstrated that it is also useful for inferring hidden dissipation of timescale-separated systems when having access to only slow variables [19,20]. Other related theoretical generalization can be found in [21–24].

Although the HS equality seems very general, its validity remains unclear for *discrete* Markov processes. In this context, Lippiello *et al.* have shown that the HS equality is recovered when entropy production in the environment is small for each jump [25]. A central assumption there is that the forward and backward transition rates respond *symmetrically* to the external perturbation. However, this symmetry is violated for molecular motors, according to recent experimental and modeling work [26–31]. Furthermore, various forms of generalized FDT that go beyond symmetric perturbation reveal non-trivial dependence on the asymmetry [10,32,33], in sharp contrast with the simplicity of the HS equality.

Here, we clarify the connection between dissipation rate and violation of the FDT for Markov systems with perturbation asymmetry. We find surprisingly that the FDT is violated even in the high-frequency limit, leading to a divergent FDT violation integral, although the dissipation rate remains finite. We propose two renormalization schemes to remove the divergence of the FDT violation integral, and show that the renormalized integrals well predict the dissipation rate when the entropic change per jump is small. The main results are illustrated with a minimum model for kinesin.

II. GENERAL MARKOV SYSTEMS

Consider a general Markov process with N states. The transition from state n to state m ($1 \leqslant n, m \leqslant N$) happens with rate w_n^m. The probability $P_n(t)$ at state n and time t evolves

―――――――――
[*]wangsw09@csrc.ac.cn

according to the following master equation:

$$\frac{d}{dt}P_n(t) = \sum_m M_{nm}P_m(t), \qquad (3)$$

where M is assumed to be an irreducible transition rate matrix determined by $M_{nm} = w_m^n - \delta_{nm}\sum_k w_m^k$ with δ_{nm} being the Kronecker delta. The jth left and right eigenmodes, denoted as $x_j(n)$ and $y_j(n)$, respectively, satisfy the characteristic equations $\sum_m M_{nm}x_j(m) = -\lambda_j x_j(n)$ and $\sum_m y_j(m)M_{mn} = -\lambda_j y_j(n)$. Here, the minus sign is introduced to have an "eigenvalue" λ_j with a positive real component [34]. These eigenvalues are arranged in the ascending order by their real part, i.e., $\text{Re}(\lambda_1) \leqslant \text{Re}(\lambda_2) \leqslant \cdots$. This system has a unique stationary distribution P_m^{ss} that satisfies $\sum_m P_m^{ss} = 1$. For the ground state associated with $\lambda_1 = 0$, $y_1(n)$ should be constant and $x_1(m)$ be proportional to P_m^{ss}. Here, we fix $y_1 = 1$ and $x_1(m) = P_m^{ss}$. For this system, we can always find a set of eigenmodes that satisfy the orthogonal relations $\sum_m x_j(m)y_{j'}(m) = \delta_{jj'}$ and completeness relations $\sum_j x_j(n)y_j(m) = \delta_{nm}$, which we use in the following analysis. The left and right eigenmodes are coupled for equilibrium systems: $x_j(m) = y_j(m)P_m^{eq}$. This is not true for non-equilibrium systems.

We introduce an external perturbation h that modifies the transition rates to be

$$\tilde{w}_m^n = w_m^n \exp\left[h\left(\theta_n^m + \frac{1}{2}\right)\frac{\mathcal{Q}_n - \mathcal{Q}_m}{T}\right]. \qquad (4)$$

Here, $\mathcal{Q}_m$ is a variable conjugate to perturbation h, and θ_n^m parametrizes the asymmetry of the transition rates in response to external perturbation. θ_n^m may vary for different transitions, but should satisfy $\theta_n^m = -\theta_m^n$. $\theta_n^m = 0$ corresponds to the symmetric case. We are interested in the correlation and response spectrum of the velocity observable $\dot{Q}_t = d\mathcal{Q}_{n_t}/dt$. The strategy is to project these spectra onto the eigenspace. We introduce the projection coefficients: $\alpha_j \equiv \sum_n \mathcal{Q}_n x_j(n)$, $\beta_j \equiv \sum_n \mathcal{Q}_n y_j(n)P_n^{ss}$, and $\phi_j \equiv \sum_n B_n y_j(n)$, where B_n captures the effect from perturbation, and is given by $B_n = \sum_m (\theta_n^m J_n^m + \mathcal{A}_n^m)(\mathcal{Q}_n - \mathcal{Q}_m)/T$. Here, $\mathcal{A}_n^m \equiv (w_n^m P_n^{ss} + w_m^n P_m^{ss})/2$ is the dynamical activity between state n and m, while $J_n^m \equiv w_n^m P_n^{ss} - w_m^n P_m^{ss}$ is the net flux from state n to m. Then, we obtain

$$\tilde{C}_{\dot{Q}}(\omega) = \sum_{j=2}^N 2\alpha_j\beta_j\lambda_j\left[1 - \frac{1}{1+(\omega/\lambda_j)^2}\right], \qquad (5a)$$

$$\tilde{R}_{\dot{Q}}(\omega) = \sum_{j=2}^N \alpha_j\phi_j\left[1 - \frac{1+i(\omega/\lambda_j)}{1+(\omega/\lambda_j)^2}\right] \qquad (5b)$$

with i the imaginary unit. We have used this framework previous in the context of symmetric perturbation [19,20]. See Appendix A for more details.

Let us consider the high frequency limit first. According to Eq. (5), we have $\tilde{C}_{\dot{Q}}(\infty) = \sum_{j=2}^N 2\alpha_j\beta_j\lambda_j$ and $\tilde{R}_{\dot{Q}}(\infty) = \sum_{j=2}^N \alpha_j\phi_j$. Following the definitions of these

coefficients, we obtain

$$\tilde{C}_{\dot{Q}}(\infty) = \sum_{n,m}(\mathcal{Q}_n - \mathcal{Q}_m)^2\mathcal{A}_n^m, \qquad (6a)$$

$$\tilde{R}_{\dot{Q}}(\infty) = \frac{1}{2T}\sum_{n,m}(\mathcal{Q}_n - \mathcal{Q}_m)^2(\theta_n^m J_n^m + \mathcal{A}_n^m). \qquad (6b)$$

In obtaining Eq. 6(a), we note that $\sum_j x_j(n)\lambda_j y_j(m) = -M_{nm}$, and that any summation over the full state space is invariant under the switching of the label, i.e., $n \leftrightarrow m$. Because θ is introduced only at the stage of perturbation here, the correlation spectrum does not depend on θ. More specifically, $\tilde{C}_{\dot{Q}}(\infty)$ only depends on the activity $\mathcal{A}_n^m$, while $\tilde{R}_{\dot{Q}}(\infty)$ has an additional dependence on the flux J_n^m in the presence of an asymmetric load-sharing factor. The FDT violation in the high-frequency limit is then

$$\mathcal{V}_\infty \equiv \lim_{\omega\to\infty}[\tilde{C}_{\dot{x}}(\omega) - 2T\tilde{R}_{\dot{x}}'(\omega)] = -\sum_{n,m}\theta_m^n J_m^n(\mathcal{Q}_m - \mathcal{Q}_n)^2. \qquad (7)$$

It vanishes for any equilibrium systems ($J_m^n = 0$) or non-equilibrium systems with symmetric perturbation ($\theta_m^n = 0$). Otherwise, a finite FDT violation persists even in the high-frequency limit, which is quite surprising. When the transitions are dominated by futile back-and-forth jumps, i.e., $|\mathcal{A}_n^m| \gg |J_n^m|$, the system has a relatively small high-frequency-limit violation, i.e., $|\mathcal{V}_\infty/\tilde{C}_{\dot{Q}}(\infty)| \ll 1$. This will be the typical case when individual jumps produce a small entropic change in the environment, as will be illustrated later.

The direct consequence of a non-zero $\mathcal{V}_\infty$ is a divergent FDT violation integral I and thus complete breakdown of the HS equality (as the dissipation rate still remains finite). To get rid of divergence, we first subtract $\mathcal{V}_\infty$ from the violation spectrum and then introduce the renormalized FDT violation integral:

$$I_* \equiv \langle\dot{Q}\rangle_{ss} + \int_{-\infty}^\infty [\tilde{C}_{\dot{Q}}(\omega) - 2T\tilde{R}_{\dot{Q}}'(\omega) - \mathcal{V}_\infty]\frac{d\omega}{2\pi}. \qquad (8)$$

A more practical scheme of renormalization will be discussed towards the end. Combined with Eq. (5), we obtain $I_* = \sum_j \lambda_j\alpha_j(T\phi_j - \beta_j\lambda_j)$.[1] Using the definitions of these coefficients and summing over all eigenmodes, we obtain (see Appendix A)

$$I_* = \sum_{n,m}\left(\frac{\bar{v}_n + \bar{v}_m}{4} + \frac{\bar{v}_n - \bar{v}_m}{2}\theta_n^m\right)J_n^m(\mathcal{Q}_m - \mathcal{Q}_n), \qquad (9)$$

where $\bar{v}_n \equiv \sum_m w_n^m(\mathcal{Q}_m - \mathcal{Q}_n)$ is the average change rate of Q_t when it starts from state n. Evidently from this equation, the FDT violation only comes from transitions that change the observable $\mathcal{Q}_n$, as it should, and it is proportional to the local net flux J_n^m, the signature of non-equilibrium systems. Below, we discuss the structure of $\mathcal{V}_\infty$ and the connection between I_* and the dissipation rate $\dot{q}$ through more specific models.

---

[1]We note that $\langle\dot{Q}\rangle_{ss} = 0$ in this system due to its finite state space. However, we expect Eq. (9) to work even for systems with an infinite state space, as suggested by our analytical and numerical examples.
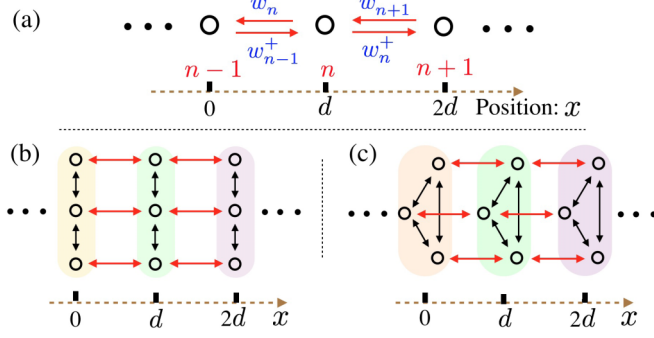
FIG. 1. (a) One-dimensional (1D) hopping process. (b),(c) Multi-dimensional hopping models. The corresponding observable $\mathcal{Q}_n$, which is x here, does not distinguish microscopic states within each colored block. As with the 1D hopping model, we assume that θ is the same for all red transitions. These models may describe molecular motors that hop along a discrete lattice with several internal chemical states. They also resemble sensory adaptation model in E. coli [35].

III. APPLICATION TO VARIOUS MODELS

Consider a particle hopping along a discrete lattice with a lattice constant d, as illustrated in Fig. 1(a). Each state n has a well-defined energy U_n. The transition rates are assumed to satisfy

$$w_n^+ = w_0 \exp\left(\left(\theta + \frac{1}{2}\right)\frac{\Delta U_n + hd}{T}\right), \quad (10a)$$

$$w_{n+1}^- = w_0 \exp\left(\left(\theta - \frac{1}{2}\right)\frac{\Delta U_n + hd}{T}\right) \quad (10b)$$

with w_0 the constant prefactor, and $\Delta U_n \equiv U_n - U_{n+1}$ the dissipation per jump. This model satisfies local detailed balance, i.e., $w_n^+/w_{n+1}^- = \exp([\Delta U_n + hd]/T)$. We assume that U_n is constructed from a continuous function $U(x)$ via $U_n = U(nd)$. The energy landscape can be tilted to drive the system out of equilibrium.

First, we derive the high-frequency violation $\mathcal{V}_\infty$. For this system, the conjugate observable $\mathcal{Q}_n$ is position x. We note that $(\mathcal{Q}_m - \mathcal{Q}_n)^2 = d^2$ for all allowed transitions. Furthermore, both the flux $J = \langle \dot{x} \rangle_{ss}/L$ and the asymmetric factor θ are constant in the state space. Therefore, Eq. (7) is reduced to

$$\mathcal{V}_\infty = -2\theta\langle \dot{x} \rangle_{ss} d. \quad (11)$$

This simple relation (11) can be easily generalized to multi-dimensional hopping processes illustrated in Fig. 1(b),(c), by lumping states within each colored block and fluxes between two connected blocks. For such multi-dimensional models, $\mathcal{V}_\infty$ may vanish even if the system remains out of equilibrium, as $\langle \dot{x} \rangle_{ss} = 0$ is not a sufficient condition for equilibrium here. This is not possible for one-dimensional (1D) systems.

Second, we derive the renormalized HS equality. According to I_* in Eq. (9), we have

$$I_* = d \sum_n \left(\frac{\bar{v}_n + \bar{v}_{n+1}}{2} + \theta(\bar{v}_n - \bar{v}_{n+1})\right)J_n^{n+1}. \quad (12)$$

Here, $\bar{v}_n = d(w_n^+ - w_n^-)$. We introduce $\epsilon_n \equiv \ln[w_n^+/w_{n+1}^-]$ as the entropy produced in the environment per jump, which has

a characteristic amplitude ϵ. Expanding Eq. (12) in Taylor series of ϵ, we have $\bar{v}_n + \bar{v}_{n+1} = 2w_0 d\epsilon_n + \theta\, O(\epsilon^2) + O(\epsilon^3)$ and $\bar{v}_n - \bar{v}_{n+1} = O(\epsilon^2)$ (see Appendix B), which gives

$$I_* = w_0 d^2 \sum_n J_n^{n+1}\epsilon_n(1 + \theta\, O(\epsilon) + O(\epsilon^2)). \quad (13)$$

We identify $\dot{q} = T\sum_n J_n^{n+1}\epsilon_n$ as the dissipation rate of the stochastic trajectory Q_t, and $\gamma_* = T/(w_0 d^2)$ as the effective friction coefficient. Finally, we obtain

$$\gamma_* I_* = \dot{q}(1 + \theta\, O(\epsilon) + O(\epsilon^2)). \quad (14)$$

The renormalized HS equality, i.e., $\gamma_* I_* = \dot{q}$, is recovered when ϵ is small, regardless of asymmetry and discreteness. While the asymmetry leads to a first order deviation, the deviation of discreteness is only of the second order, thus much smaller. The assumption of a constant θ is crucial here. Throughout the derivation, we did not assume that J_n^{n+1} is constant, a characteristic property of 1D systems. Hence, Eq. (14) can be generalized to multi-dimensional models in Fig. 1(b),(c), where the same value of $\mathcal{Q}_p = pd$ is shared by all the states within the same colored block.

We sketch the generalization here. The perturbed rates of the *red* transitions that change the observable are assumed to satisfy

$$\tilde{w}_m^n = w_0 \exp\left(\left(\theta + \frac{1}{2}\right)\left[\epsilon_m^n + h\frac{\mathcal{Q}_n - \mathcal{Q}_m}{T}\right]\right), \quad (15a)$$

$$\tilde{w}_n^m = w_0 \exp\left(\left(\theta - \frac{1}{2}\right)\left[\epsilon_m^n + h\frac{\mathcal{Q}_n - \mathcal{Q}_m}{T}\right]\right), \quad (15b)$$

which essentially mimics Eq. (10), except that we do not assume an energy landscape U_n. The dissipation rate through the stochastic trajectory Q_t is defined to be

$$\dot{q} \equiv T \sum_{n,m}(1 - \delta_{\mathcal{Q}_n\mathcal{Q}_m})J_n^m\epsilon_n^m, \quad (16)$$

where $\epsilon_n^m = \ln[\omega_n^m/\omega_m^n]$ is the environment's entropy production for the transition from state n to m, and $(1 - \delta_{\mathcal{Q}_n\mathcal{Q}_m})$ is a weight that only counts transitions that change the observable. Assuming that both ϵ_n^m and its relative variation are small along the direction of red transitions, the renormalized HS equality also emerges. The differences of network topologies are captured by the effective friction coefficient $\gamma_* = 4T/(kw_0 d^2)$, with k being the number of red transitions out of a node.

IV. MINIMUM MODEL FOR KINESIN

A kinesin is a type of molecular motor that, powered by ATP, moves along microtubule filaments. Following the experimental and modeling work in [30], we use the biased diffusive model presented in Fig. 2(a) to describe the stepwise dynamics of this motor, with d the step size. This is a special case of the 1D hopping model that has translational invariance. The dissipation per jump ΔU can be tuned by changing ATP concentration, and h is the external force that is applied to the bead attached to the motor in a typical experimental setup. Experiments show that the external force only affects the forward transition rate w_+ [30], as illustrated in Fig. 2(b). This situation occurs when the external force only varies the energy barrier
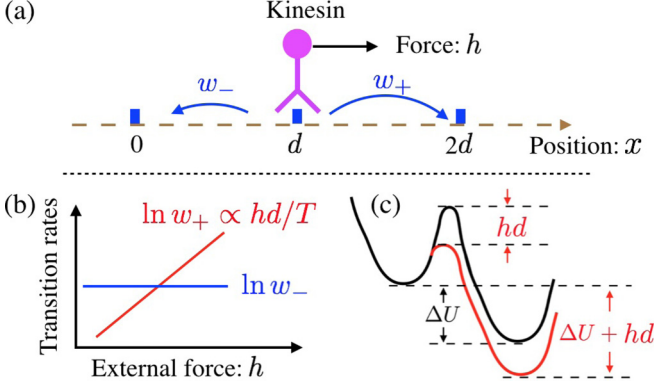
FIG. 2. (a) A simplified Markov model for kinesin. (b) The experimentally suggested relations between transition rates $w_\pm$ and the external force h [30], corresponding to the case with $\theta = 0.5$. (c) The energy landscape connecting neighboring states. The external force only varies the energy barrier for the forward transition.

for the forward transition [Fig. 2(c)]. The scenario of kinesin corresponds to a completely asymmetric model with $\theta = 0.5$.

This simple model allows analytical solutions. At the steady state with $h = 0$, the average velocity is given by $\langle \dot{x} \rangle_{ss} = d(w_+ - w_-)$, and the dissipation rate $\dot{q} = \Delta U \langle \dot{x} \rangle_{ss}/d = \Delta U(w_+ - w_-)$. The correlation spectrum of the velocity $\dot{x}$ is found to be $\tilde{C}_{\dot{x}}(\omega) = (\omega_+ + \omega_-)d^2$, while the response spectrum of the velocity, measured via applying a small and periodic force, is given by $\tilde{R}_{\dot{x}}(\omega) = d^2[2\theta(w_+ - w_-) + (w_+ + w_-)]/2T$. These spectra are constant in the frequency domain due to the translational invariance of this simple model. Indeed, the FDT is violated even in the high frequency limit due to the presence of asymmetry, as illustrated in Fig. 3(a).
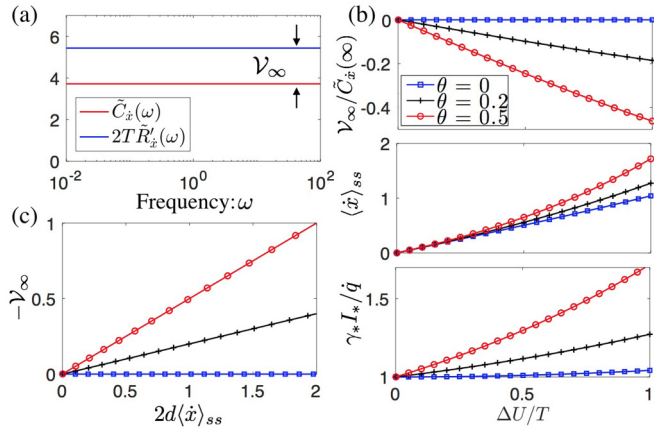

FIG. 3. (a) The correlation spectrum $\tilde{C}_{\dot{x}}(\omega)$ and the (real part of) response spectrum $\tilde{R}'_{\dot{x}}(\omega)$ for the velocity $\dot{x}_t$, obtained at $\Delta U = 1$ and $\theta = 0.5$. A finite violation of FDT, $\mathcal{V}_\infty$, persists even in the high frequency limit. (b) The relative violation of the FDT in the high-frequency limit $[\mathcal{V}_\infty/\tilde{C}_{\dot{x}}(\infty)]$, the average drifting velocity $\langle \dot{x} \rangle_{ss}$, and the predicted dissipation rate $\gamma_* I_*$ based on the renormalized FDT violation integral against the actual dissipation rate $\dot{q}$. Here, the control parameter is the entropic change per jump, i.e., $\Delta U/T$. (c) Verification of Eq. (11). The slope of each curve gives corresponding θ. Other parameters: $w_0 = 1$, $d = 1$, and $h = 0$.

The relative high-frequency violation $\mathcal{V}_\infty/\tilde{C}_{\dot{x}}(\infty)$ becomes smaller when the entropic change per transition, i.e., $\Delta U/T$, decreases [Fig. 3(b)]. It can be checked easily that Eq. (11) holds here, as illustrated in Fig. 3(c). Therefore, a smaller driving energy ΔU reduces $\mathcal{V}_\infty$ by slowing down the biased motion [Fig. 3(b)]. Such a violation has been noticed recently in a more realistic model of kinesin [31]. For a small $\Delta U/T$, the renormalized FDT violation integral I_* multiplied with the effective friction γ_* well predicts the dissipation rate $\dot{q}$, as shown in Fig. 3(b).

V. PRACTICAL RENORMALIZATION

An important parameter in applying the HS equality is the ambient temperature T, which is very challenging to determine (or control) experimentally due to the tiny size of the molecular machine. In practice, T has been determined from the ratio $\tilde{C}_{\dot{x}}(\omega)/2\tilde{R}'_{\dot{x}}(\omega)$ in the high-frequency regime, assuming that FDT is satisfied there [17,18,31]. According to our current study, this assumption might be wrong in the presence of perturbation asymmetry. In fact, the high-frequency violation leads to a modified temperature:

$$T_{re} \equiv \lim_{\omega \to \infty} \frac{\tilde{C}_{\dot{x}}(\omega)}{2\tilde{R}'_{\dot{x}}(\omega)} = \frac{T}{1 - \mathcal{V}_\infty/\tilde{C}_{\dot{x}}(\infty)}. \quad (17)$$

It is reduced to the bath temperature when $\mathcal{V}_\infty = 0$. With this temperature, we obtain a renormalized FDT violation integral that becomes well-behaved:

$$I_{re} \equiv \langle \dot{x} \rangle_{ss}^2 + \int_{-\infty}^{\infty} [\tilde{C}_{\dot{x}}(\omega) - 2T_{re}\tilde{R}'_{\dot{x}}(\omega)] \frac{d\omega}{2\pi}. \quad (18)$$

The effective friction coefficient γ_{re} can be determined from

$$\gamma_{re} \equiv \lim_{\omega \to \infty} \frac{1}{\tilde{R}'_{\dot{x}}(\omega)}, \quad (19)$$

which is an exact relation for Langevin systems, and serves as a generalization here. When the entropic change per jump is small, we have $\mathcal{V}_\infty/\tilde{C}_{\dot{x}}(\infty) \ll 1$, thus $I_{re} \approx I_*$ and $\gamma_{re} \approx \gamma_*$. Therefore, $\gamma_{re} I_{re}$ also becomes a reasonable estimation of the dissipation rate $\dot{q}$ when the entropic change per jump is small.

We provide a numerical illustration for this renormalization scheme using the 1D hopping model. Consider that $U(x) = U(x + L) + \Delta\mu$ is a periodic function tilted by an energy input $\Delta\mu$ at each period L, which drives the system out of equilibrium. This is illustrated in Fig. 4(a). The number of states within each period is $N = L/d$. The prefactor w_0 scales with $1/d^2$ so that the global features (mean velocity, etc.) converge to a finite value in the continuum limit $d/L \to 0$. The correlation and response spectrum are shown in Fig. 1(b) for $d = 0.1$ and $\theta = -0.2$. Again, the FDT violation persists even in the high frequency limit. The average entropy production in the environment per jump, $\frac{1}{N} \sum_n |\Delta U_n/T|$, is a crucial parameter here. It roughly scales with the discreteness d of the system, and vanishes in the limit $d/L \to 0$. By changing the discreteness in our numerical simulation, we find that, below a sufficiently small $\frac{1}{N} \sum_n |\Delta U_n/T|$, the relative high-frequency FDT violation becomes negligible [Fig. 4(c)], and the renormalized HS equality based on the modified temperature emerges [Fig. 4(d)]. This holds true for various values of θ. Again, $\theta = 0$ is special in that the
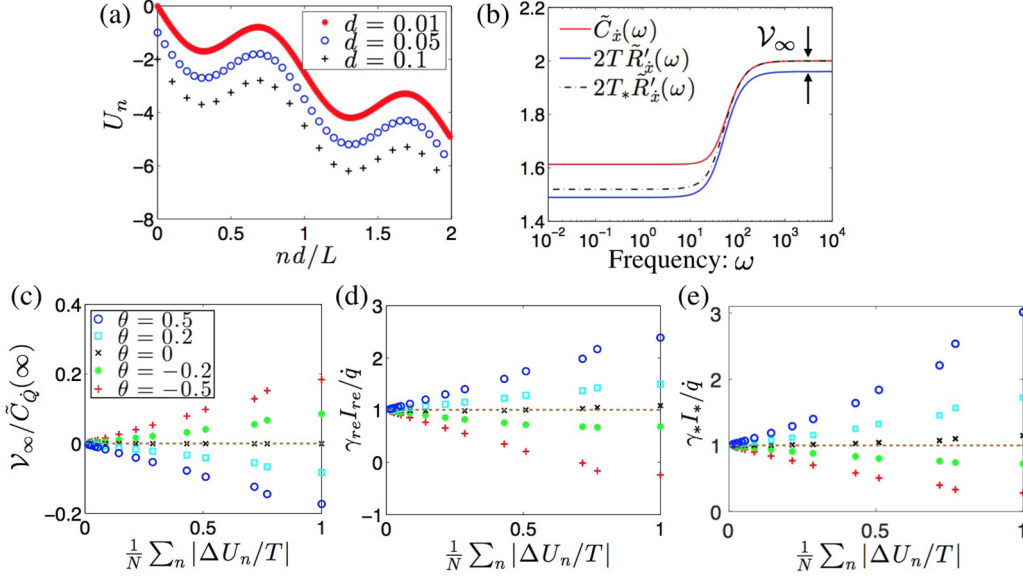
FIG. 4. (a) The energy landscape U_n for the 1D hopping model, constructed from $U(x) = -\sin(2\pi x/L) - \Delta\mu x/L$ at a given lattice constant d. The landscapes for different d's are shifted vertically for illustration. (b) The correlation and response spectrum for the velocity $\dot{x}_t \equiv \dot{n}_t d$, obtained at $d = 0.1$ and $\theta = -0.2$. The FDT is restored in the high frequency limit with the renormalized temperature. (c) The relative high-frequency-limit violation of FDT against the average entropic change in the environment per jump: $\frac{1}{N}\sum_n |\Delta U_n/T|$. (d),(e) Emergence of the renormalized HS equality (from different schemes) at small medium entropy production per jump. Other parameters: $w_0 = 1/d^2$, $T = 1$, $L = 1$, $\Delta\mu = 2.5$, and $h = 0$.

corresponding $\mathcal{V}_\infty = 0$, and $\gamma_{re}I_{re}$ proves to be a much more accurate (though not exact) estimation for the dissipation rate $\dot{q}$ [Fig. 4(d)].

The performance for the previous renormalization scheme is also shown in Fig. 4(e), which is quite similar. Hence, under a small medium entropy production per step (i.e., $\epsilon \ll 1$), different renormalization schemes converge to the same correct answer since $\mathcal{V}_\infty/\tilde{C}_{\dot{Q}} \to 0$ in the limit $\epsilon \to 0$. However, the original HS equality still breaks down due to the divergence of the FDT violation integral I.

VI. CONCLUSION

We have demonstrated for Markov systems that the FDT violation persists generally in the high frequency limit in the presence of asymmetric perturbation. This is in sharp contrast to our physical intuition that the high-frequency correlation and response essentially reflect only the thermal property of the bath. The high-frequency violation leads to a divergent FDT violation integral that invalidates the HS equality. However, proper renormalization of the FDT violation integral restores the HS equality effectively when the entropic change in the environment is small for each jump. Hence, our study provides a protocol to estimate the dissipation rate for discrete Markov systems with asymmetry, based on the measured correlation and response spectra. Our study also reveals a linear relation between the high-frequency-limit violation and the asymmetric factor θ, and therefore can be exploited to infer θ experimentally. We believe that our results will guide further investigation of kinesin [31].

ACKNOWLEDGMENTS

APPENDIX A: CORRELATION, RESPONSE, AND FDT VIOLATION IN GENERAL MARKOV MODELS

1. Correlation spectrum

Noting that the correlation function for Q_t satisfies $C_Q(t - \tau) \equiv \langle [Q_t - \langle Q \rangle_{ss}][Q_\tau - \langle Q \rangle_{ss}] \rangle_{ss}$, we have

$$C_{\dot{Q}}(t - \tau) = \frac{\partial^2 C_Q(t - \tau)}{\partial \tau \, \partial t}. \tag{A1}$$

It is easier to calculate $C_Q(t - \tau)$ first. Assuming $t \geqslant \tau$, it satisfies

$$C_Q(t - \tau) = \sum_{n,n'} \mathcal{Q}_n \mathcal{Q}_{n'} P(t - \tau; n, n') P_{n'}^{ss} - \langle Q \rangle_{ss}^2, \tag{A2}$$

where $P(t - \tau; n, n')$ is the propagator, or the probability for reaching state n at time t, assuming that the system starts from state n' at time τ. In the eigenspace,

$$P(t - \tau; n, n') = \sum_j y_j(n') e^{-\lambda_j |t - \tau|} x_j(n). \tag{A3}$$

Indeed, it is the solution of the corresponding master equation (3), given the initial condition $P(0; n, n') = \delta_{nn'}$. Inserting this relation back to Eq. (A2) and introducing the projection of $\mathcal{Q}$ on the jth eigenmode, i.e., $\alpha_j \equiv \sum_n \mathcal{Q}_n x_j(n)$ and $\beta_j \equiv \sum_n \mathcal{Q}_n y_j(n) P_n^{ss}$, we obtain the expansion of correlation function in the eigenspace:

$$C_Q(t - \tau) = \sum_{j=2}^N \alpha_j \beta_j e^{-\lambda_j |t - \tau|}. \tag{A4}$$

The contribution of the first eigenmode is counteracted by $\langle Q \rangle_{ss}^2$. Stationarity of the system guarantees that $C_Q(t - \tau) = C_Q(\tau - t)$. Therefore, Eq. (A4) obtained from $t \geqslant \tau$ is also applicable for $t < \tau$. We use the following convention for Fourier transform:

$$\tilde{f}(\omega) = \int_{-\infty}^{\infty} f(t) \exp(i\omega t) dt, \tag{A5}$$

$$f(t) = \int_{-\infty}^{\infty} \tilde{f}(\omega) \exp(-i\omega t) \frac{d\omega}{2\pi}. \tag{A6}$$

Combining Eq. (A1), Fourier transformation and Eq. (A4), we finally obtain the velocity correlation spectrum 6(a).

2. Response spectrum

The response spectrum can be obtained by studying the response of the system to a periodic perturbation. Consider $h_t = h_0 \exp(-i\omega t)$ with h_0 a small amplitude and i the imaginary unit. Expanded in Taylor series, the modified transition rate matrix $\tilde{M}$ is given by

$$\tilde{M} = M + M^* h_0 \exp(-i\omega t) + O(h_0^2), \tag{A7}$$

where $M^* \equiv \partial_h \tilde{M}|_{h \to 0}$. On the other hand, the modified distribution can also be expanded up to the first order:

$$\tilde{P}_m = P_m^{ss} + P_m^* h_0 \exp(-i\omega t) + O(h_0^2) \tag{A8}$$

with $P_m^* \equiv \partial_h \tilde{P}_m|_{h \to 0}$. Since $d\tilde{P}_m/dt = \sum_n \tilde{M}_{mn} \tilde{P}_n$ and $\sum_n M_{mn} P_n^{ss} = 0$, we obtain in a matrix form

$$P^* = -\frac{1}{M + i\omega} M^* P^{ss}. \tag{A9}$$

For the observable Q_t, its response spectrum is given by

$$\tilde{R}_Q(\omega) = \sum_n \mathcal{Q}_n P_n^* = \sum_{j=2}^{N} \frac{\alpha_j \phi_j}{\lambda_j - i\omega}, \tag{A10}$$

where $\phi_j \equiv \sum_n B_n y_j(n)$ with $B_n \equiv \sum_m M_{nm}^* P_m^{ss}$. By using the transformation $R_{\dot{Q}}(t) = dR_Q/dt$ or $\tilde{R}_{\dot{Q}}(\omega) = -i\omega \tilde{R}_Q(\omega)$, we obtain the velocity response spectrum 6(b).

3. The renormalized FDT violation integral I_*

We derive Eq. (9). First, note that $(T\phi_j - \lambda_j \beta_j)$ is a key quantity in the violation spectrum integral:

$$I_* = \sum_j \lambda_j \alpha_j (T\phi_j - \beta_j \lambda_j).$$

According to definitions of these coefficients, we obtain

$$T\phi_j - \lambda_j \beta_j = \sum_{n,m} y_j(n) J_m^n \left(\frac{\mathcal{Q}_n + \mathcal{Q}_m}{2} + \theta_n^m (\mathcal{Q}_m - \mathcal{Q}_n) \right).$$

For equilibrium systems, the flux J_m^n vanishes due to detailed balance. This leads to $T\phi_j = \beta_j \lambda_j$ for all eigenmodes, and thus the vanishing of the FDT violation integral. On the other hand, $\lambda_j \alpha_j = -\sum_n \bar{v}_n x_j(n)$, with $\bar{v}_n \equiv \sum_m w_n^m (\mathcal{Q}_m - \mathcal{Q}_n)$ being the average change rate of Q_t when it starts from state n.

Combining these relations, we obtain the analytical expression for the effective FDT violation integral:

$$I_* = \sum_{n,m} \bar{v}_n J_n^m \left(\frac{\mathcal{Q}_n + \mathcal{Q}_m}{2} + \theta_n^m (\mathcal{Q}_m - \mathcal{Q}_n) \right). \tag{A11}$$

Noting that $\sum_m J_n^m = 0$ due to stationarity, we can subtract $\sum_{n,m} \bar{v}_n J_n^m \mathcal{Q}_n$ (which is also zero) from I_*, and symmetrize the resulting expression to obtain Eq. (9).

APPENDIX B: THE RENORMALIZED HS EQUALITY

Here, we provide more details of deriving the renormalized HS equality, give numerical illustrations, and present the generalization to higher dimensional models mentioned in the Main Text. First, we consider the 1D hopping model mentioned in Fig. 1(a). Following Eq. (12), we are interested in how $\bar{v}_n + \bar{v}_{n+1}$ and $\bar{v}_n - \bar{v}_{n+1}$ behave when ϵ_n is small. Here, $\bar{v}_n = d(w_n^+ - w_n^-)$. More explicitly, we have

$$\bar{v}_n + \bar{v}_{n+1} = w_0 d [(e^{(\theta+1/2)\epsilon_n} - e^{(\theta-1/2)\epsilon_{n-1}}) + (e^{(\theta+1/2)\epsilon_{n+1}} - e^{(\theta-1/2)\epsilon_n})].$$

Applying Taylor expansion, we obtain

$$\bar{v}_n + \bar{v}_{n+1} = w_0 d \left[\epsilon_n + \frac{\epsilon_{n-1} + \epsilon_{n+1}}{2} + \theta(\epsilon_{n+1} - \epsilon_{n-1}) \right.$$
$$+ \theta \left(\epsilon_n^2 + \frac{\epsilon_{n+1}^2 + \epsilon_{n-1}^2}{2} \right)$$
$$\left. + \left(\frac{1}{8} + \frac{1}{2}\theta^2 \right) (\epsilon_{n+1}^2 - \epsilon_{n-1}^2) + O(\epsilon^3) \right]$$

with ϵ capturing the overall amplitude of ϵ_n. Similarly, we have

$$\bar{v}_n - \bar{v}_{n+1} = w_0 d \left[\frac{\epsilon_{n-1} - \epsilon_{n+1}}{2} + 2\theta \left(\epsilon_n - \frac{\epsilon_{n+1} + \epsilon_{n-1}}{2} \right) \right.$$
$$+ \left(\frac{1}{4} + \theta^2 \right) \left(\epsilon_n^2 - \frac{\epsilon_{n-1}^2 + \epsilon_{n+1}^2}{2} \right)$$
$$\left. - \frac{\theta}{2} (\epsilon_{n+1}^2 - \epsilon_{n-1}^2) + O(\epsilon^3) \right].$$

Now, we assume $\epsilon_n = \epsilon f(nd)$ with $f(x)$ a continuous function and $\epsilon \propto d$. The motivation of this assumption is that there is an underlying smooth energy landscape, as discussed in the main text. From a Taylor expansion, we obtain

$$\epsilon_{n\pm 1} = \epsilon \left[f(nd) \pm \frac{\partial f}{\partial x} d + \frac{1}{2} \frac{\partial^2 f}{\partial x^2} d^2 + O\left(\frac{d^3}{L^3} \right) \right].$$

Therefore, we have

$$\epsilon_{n+1} + \epsilon_{n-1} = 2\epsilon_n + O\left(\epsilon \frac{d^2}{L^2} \right), \tag{B1}$$

$$\epsilon_{n+1} - \epsilon_{n-1} = 2\epsilon \frac{\partial f}{\partial x} d + O\left(\epsilon \frac{d^3}{L^3} \right), \tag{B2}$$

$$\epsilon_{n+1}^2 + \epsilon_{n-1}^2 = 2\epsilon_n^2 + O\left(\epsilon^2 \frac{d^2}{L^2} \right), \tag{B3}$$

$$\epsilon_{n+1}^2 - \epsilon_{n-1}^2 = 4\epsilon_n \frac{\partial f}{\partial x} d + O\left(\epsilon^2 \frac{d^3}{L^3} \right). \tag{B4}$$

Plugging these relations back into the Taylor expansion of $\bar{v}_n + \bar{v}_{n+1}$ and $\bar{v}_n - \bar{v}_{n+1}$, and noting that $d/L = O(\epsilon)$, we finally obtain

$$\bar{v}_n + \bar{v}_{n+1} = 2w_0 d(\epsilon_n + \theta\, O(\epsilon^2) + O(\epsilon)^3), \tag{B5}$$

$$\bar{v}_n - \bar{v}_{n+1} = O(\epsilon^2). \tag{B6}$$

This then leads to Eq. (14).

[1] S. Toyabe and M. Sano, J. Phys. Soc. Jpn. **84**, 102001 (2015).
[2] I. A. Martínez, É. Roldán, L. Dinis, and R. A. Rica, Soft Matter **13**, 22 (2017).
[3] S. Ciliberto, Phys. Rev. X **7**, 021051 (2017).
[4] R. Kubo, Rep. Prog. Phys. **29**, 255 (1966).
[5] L. F. Cugliandolo, D. S. Dean, and J. Kurchan, Phys. Rev. Lett. **79**, 2168 (1997).
[6] L. F. Cugliandolo, J. Kurchan, and L. Peliti, Phys. Rev. E **55**, 3898 (1997).
[7] P. Martin, A. Hudspeth, and F. Jülicher, Proc. Natl. Acad. Sci. USA **98**, 14380 (2001).
[8] D. Mizuno, C. Tardin, C. Schmidt, and F. MacKintosh, Science **315**, 370 (2007).
[9] M. Baiesi, C. Maes, and B. Wynants, Phys. Rev. Lett. **103**, 010602 (2009).
[10] U. Seifert and T. Speck, Europhys. Lett. **89**, 10007 (2010).
[11] M. Baiesi and C. Maes, New J. Phys. **15**, 013004 (2013).
[12] T. Speck and U. Seifert, Europhys. Lett. **74**, 391 (2006).
[13] J. Prost, J.-F. Joanny, and J. M. R. Parrondo, Phys. Rev. Lett. **103**, 090601 (2009).
[14] T. Harada and S.-I. Sasa, Phys. Rev. Lett. **95**, 130602 (2005).
[15] T. Harada and S.-I. Sasa, Phys. Rev. E **73**, 026131 (2006).
[16] T. Harada and S.-I. Sasa, Math. Biosci. **207**, 365 (2007).
[17] S. Toyabe and E. Muneyuki, New J. Phys. **17**, 015008 (2015).
[18] S. Toyabe, T. Okamoto, T. Watanabe-Nakayama, H. Taketani, S. Kudo, and E. Muneyuki, Phys. Rev. Lett. **104**, 198103 (2010).
[19] S.-W. Wang, K. Kawaguchi, S.-I. Sasa, and L.-H. Tang, Phys. Rev. Lett. **117**, 070601 (2016).
[20] S.-W. Wang, K. Kawaguchi, S.-I. Sasa, and L.-H. Tang, arXiv:1610.00120 (2016).
[21] J. M. Deutsch and O. Narayan, Phys. Rev. E **74**, 026112 (2006).
[22] É. Fodor, C. Nardini, M. E. Cates, J. Tailleur, P. Visco, and F. van Wijland, Phys. Rev. Lett. **117**, 038103 (2016).
[23] C. Nardini, É. Fodor, E. Tjhung, F. van Wijland, J. Tailleur, and M. E. Cates, Phys. Rev. X **7**, 021007 (2017).
[24] H. Teramoto and S.-I. Sasa, Phys. Rev. E **72**, 060102 (2005).
[25] E. Lippiello, M. Baiesi, and A. Sarracino, Phys. Rev. Lett. **112**, 140602 (2014).
[26] E. Zimmermann and U. Seifert, New J. Phys. **14**, 103023 (2012).
[27] K. Kawaguchi, S.-I. Sasa, and T. Sagawa, Biophys. J. **106**, 2450 (2014).
[28] E. Zimmermann and U. Seifert, Phys. Rev. E **91**, 022709 (2015).
[29] A. I. Brown and D. A. Sivak, Proc. Natl. Acad. Sci. USA **114**, 11057 (2017).
[30] Y. Taniguchi, M. Nishiyama, Y. Ishii, and T. Yanagida, Nat. Chem. Biol. **1**, 342 (2005).
[31] T. Ariga, M. Tomishige, and D. Mizuno, arXiv:1704.05302 (2017).
[32] G. Diezemann, Phys. Rev. E **72**, 011104 (2005).
[33] C. Maes and B. Wynants, Markov Process. Relat. **16**, 45 (2010).
[34] N. G. Van Kampen, *Stochastic Processes in Physics and Chemistry* (Elsevier, New York, 1992), Vol. 1.
[35] S.-W. Wang, Y. Lan, and L.-H. Tang, J. Stat. Mech. (2015) P07025.